

Gypsum based mixes for conservation purposes: evaluation of microstructural and mechanical features

V. Brunello^a✉, D. Bersani^d, L. Rampazzi^{b,e}, A. Sansonetti^b, C. Tedeschi^c

a. Dipartimento di Scienza ed Alta Tecnologia (DISAT), Università degli Studi dell'Insubria, (Como, Italy)

b. Istituto di Scienze del Patrimonio Culturale (ISPC-CNR), (Milano, Italy)

c. Politecnico di Milano, Dipartimento di Ingegneria Civile e Ambientale (DICA), (Milano, Italy)

d. Dipartimento di Scienze Matematiche, Fisiche e Informatiche, University of Parma (Parma, Italy)

e. Dipartimento di Scienze Umane e dell'Innovazione per il Territorio (DiSUIT), Università degli Studi dell'Insubria, (Como, Italy)

✉ valentina.brunello@uninsubria.it

Received 08 April 2019

Accepted 27 August 2019

Available on line 13 February 2020

ABSTRACT: This paper presents the study of four gypsum mixtures, focusing on the role of both inorganic and organic additives and on the micro-structural features and mechanical properties. Additives have been chosen among those most reported in historical recipes, for example magnesia, lime putty, rabbit glue. The selected mixes refer to gypsum-based materials used in artworks manufacture, such as plasters, mouldings, stuccoworks, *pastiglia*. Blank reference materials were prepared on purpose according to the specific recipe, in order to verify the final composition and to highlight the hardening mechanisms and the formation of setting compounds. The chemical composition was related to workability properties and final mechanical resistance and the action of additives as retardants was studied with interesting results. For instance, MgO imparts good properties to the mechanical features, especially with regard to the compressive strength characteristics.

KEYWORDS: Gypsum; Magnesium oxide; Compressive strength; Pore size distribution; Microstructure.

Citation/Citar como: Brunello, V.; Bersani, L.; Rampazzi, L.; Sansonetti, A.; Tedeschi, C. (2020) Gypsum based mixes for conservation purposes: evaluation of microstructural and mechanical features. *Mater. Construcc.* 70 [337], e207. <https://doi.org/10.3989/mc.2020.05019>

RESUMEN: *Mezclas basadas en yeso para su aplicación en conservación: evaluación de sus propiedades microestructurales y mecánicas.* En este artículo se han analizado cuatro mezclas basadas en yeso y se ha estudiado la influencia de los aditivos utilizados para su preparación, tanto orgánicos como inorgánicos, sobre las propiedades mecánicas y microestructurales de los materiales resultantes. Los aditivos utilizados se seleccionaron en base a aquellos que han sido principalmente publicados en recetas históricas, tales como magnesia, cal o cola de conejo. Por su parte, las mezclas basadas en yeso se eligieron en base aquellas principalmente utilizadas en obras de arte, incluyendo escayolas, molduras, estucados o *pastiglia*. También se prepararon materiales de referencia (control), de acuerdo a una mezcla específica, para verificar la composición química de las diferentes mezclas preparadas y comparar sus mecanismos de endurecimiento y formación. La composición química de los materiales preparados se ha correlacionado con su trabajabilidad y resistencia mecánica. Además, se estudió la acción retardante de los aditivos utilizados con interesantes resultados. Por ejemplo, el MgO confiere buenas propiedades mecánicas al material, especialmente en lo que se refiere a la resistencia a la compresión.

PALABRAS CLAVE: Yeso; Óxido de magnesio; Resistencia a la Compresión; Distribución de tamaño de poro; Microestructura.

ORCID ID: V. Brunello (<https://orcid.org/0000-0001-9789-7245>); D. Bersani (<https://orcid.org/0000-0002-8026-983X>); L. Rampazzi (<https://orcid.org/0000-0002-7032-8955>); A. Sansonetti (<https://orcid.org/0000-0003-4938-1417>); C. Tedeschi (<https://orcid.org/0000-0002-1718-1632>).

Copyright: © 2020 CSIC. This is an open-access article distributed under the terms of the Creative Commons Attribution 4.0 International (CC BY 4.0) License.

1. INTRODUCTION

Gypsum is a building material that has been used over the centuries since the Egyptian civilization and still presents a major role in current building technologies (1–3). Gypsum based materials were utilised in plastering and rendering, bedding mortars, stuccoworks and some outstanding decoration techniques of small artworks, such as *pastiglia*. This Italian term recalls a low-relief decoration present in several early Renaissance caskets, paintings and frames, with gilt or painted finishes. Gypsum had also a special role in prototyping techniques. The use of this material in plaster coatings was mainly due to its fireproofing, thermal and acoustic qualities, its low cost and ease of preparation (4–7). Choices in stuccoworks making, for example low and high reliefs, mouldings and *in the round* statues implied the workability properties of the mixes used. For these reasons gypsum was often mixed with both organic and inorganic natural and artificial materials, such as lime putty and organic additives (8–20). The blend with animal glue and pigments was widely used in painting ground layers and in gilded artworks, especially in the south of Europe (21–23). In the techniques called *scagliola* and *pastiglia* plasticity and workability of gypsum mixes played an important role in the final restitution of tiny details and shiny surfaces (24, 25). Gypsum has been determined in literature (14–16, 26) as a component in the external renderings of Spanish and Italian buildings (27–29), nevertheless the expectations given by its low solubility in water. Its use was also important as a support and/or binding medium for mural paintings, as in many Egyptian cycles (1–3, 30).

The technology of gypseous materials allowed several working steps since very early stages, to modern industrial processes; in fact, gypsum is formed in nature in sedimentary evaporative depositional environment. To use gypsum as a binder, thermal dehydration is required. This process starts at a temperature of 42°C, but decomposition is slow. So a range of temperature between 100°–140°C is normally used in industrial processes in a wet environment. The product of the dehydration is bassanite ($\text{CaSO}_4 \cdot \frac{1}{2}\text{H}_2\text{O}$), which rehydrates quickly when water is added. If gypsum is heated up to 200°C a soluble phase of anhydrite ($\gamma\text{-CaSO}_4$) is obtained, which rehydrates in presence of water too. Heating bassanite, over 360°C leads to the formation of the insoluble anhydrite phase $\beta\text{-CaSO}_4$, while $\alpha\text{-CaSO}_4$ is produced at 1180°C. Above 1375°C, the complete dissociation of anhydrous calcium sulphate into calcium oxide, sulphur dioxide and oxygen occurs. According to the literature there are still doubts about the transition conditions between one phase and the next (31–34).

Here we link the composition of gypsum based mixes with their final performances, discussing

how this type of knowledge could be useful in conservation practice, for example when the conservator has to integrate a missing part with a new paste (35). Scientific literature in the specific field is scarce, especially with regard to gypsum based traditional recipes. Mixtures tested in this paper have been prepared according to the historic recipes given by conservators' suggestions, together with the available scientific bibliography (10, 12, 13, 21, 33, 36–41)

2. MATERIALS AND METHODS

2.1. Materials

Materials used for the mixes and the laboratory model samples are summarized below:

- Bassanite powder ($\text{CaSO}_4 \cdot 0.5\text{H}_2\text{O}$) purchased as *Gesso Alabastrino* from *CTS (Italy)*;
- lime putty aged for 48 months *Grassello Candor* 48 months (*Italy*);
- MgO powder in analytical grade supplied by *Carlo Erba*;
- Rabbit glue, supplied in pearls. The compound was soaked in demineralised water overnight, then the excess water was rinsed off and the glue was prepared by gentle heating, until the formation of a viscous solution.

Four types of mixes were prepared:

1. pure gypsum as a reference;
2. gypsum plus rabbit glue (11, 33);
3. gypsum plus MgO (33);
4. gypsum plus lime putty (11, 16, 33, 41, 42)

The amount of water was considered crucial to achieve the final performances, so its weight in each mixture was measured.

MgO was selected because it is reported by crafts handbooks as an additive that improves the mechanical performances of gypsum based pastes (33), although this effect was not yet been verified by scientific studies. It is known from the literature that magnesium could be present in lime mortars, when magnesian lime is fired in the kiln (43, 44) starting from rock raw materials with dolomite impurities (4). Lime putty was selected because, when mixed with gypsum, it forms a well-known and diffused blend utilised in stuccoes practice (11, 13, 33, 38, 41). Finally, the choice of the rabbit glue is due to the well-documented use in *scagliola* and *pastiglia* techniques, for example in the creation of altar frontals (11, 15, 41). It is worthwhile to note that magnesium oxide and calcium carbonate have been detected in recent characterisation studies (9, 11, 13, 28, 45), as well as animal glue or other protein based materials (11, 41).

The study of the final properties of gypsum based specimen has been particularly neglected in recent literature, which in fact reports only on the different type of aggregate (11, 42), the addition of fibrous materials (46), or on the blend with organic compounds (47).

The raw materials were characterized by X-ray diffraction (XRD), infrared (FTIR) and Raman spectroscopy to verify the presence of undesirable components. Bassanite is the main component of "Gesso Alabastrino", with traces of anhydrite and dolomite, probably coming from the raw materials. The purity of MgO was confirmed, while the lime putty is designated as CL 90-Q according to EN 459-1 (48). Rabbit glue showed the typical FTIR absorption peaks of collagen (49).

Mixtures were prepared at controlled environmental parameters (65% RH and 20 °C) and the same mixing conditions were ensured for each specimen, using the same mixer and same velocity. Steady curing conditions were maintained for 28 days (50% RH and 20°C) (50). The composition of the 4 mixtures are reported in Table 1. With regard to mixtures A, B and C, they are considered to be among the most widespread ones in the art technique manuals. Instead, the mixture D was chosen in order to study the effects due to the addition of MgO. A systematic survey of historical records leads to the ratios reported in Table 1. A set of preliminary tests suggested the appropriate amount of water, considering the one already present in lime putty, or in the rabbit glue. Anyway, the proper consistency was evaluated by means of a flow table.

A series of specimens were prepared, sized 160×40×40mm as required by current standards (51), with the aim to study physical and mechanical properties, together with the microstructure. The setting time and the hardening were evaluated with Vicat needle (51), the workability was estimated through the flow table method, the flexural and compressive resistance, and the linear shrinkage were measured according to current standard (51).

Flexural strength measurements were performed after 28 days, averaging the final value on a basis of three replicates. Compressive strength tests were performed after 28 days, averaging on the 6 replicates produced by the fracture of specimens used in flexural test.

2.2. Analytical methods

The raw materials and the mixtures were characterized by XRD, FTIR, and Raman Spectroscopy. The mineralogical composition after the specimen setting was analysed too, in order to understand the effects induced by the added compounds. For each specimen three replicates were carried out. X ray diffraction was carried out on powdered samples by PANalytical X'Pert PRO X-ray diffractometer, with geometry goniometer θ - θ . The diffractograms were recorded between 3° and 75° 2 θ with a scanning speed of 0.21 θ /sec, using a Cu K α radiation, a PW generator 3040/60 in the conditions of 40kV and 40mA, and a solid-state multi-detector X'Celerator PW3015/20, with Ni filter. The powdered samples were deposited on a ground glass support. Results were interpreted by the use of the X'Pert HighScore software.

A Micro-Raman spectrometer Horiba Jobin-Yvon LabRam was used, coupled to a confocal microscope Olympus BH-4 equipped with motorized XY stage. The instrument works with two laser lines: 632.8 nm (He-Ne, 20 mW) and 473.1 nm (Nd:YAG laser, 100mW). The Raman signal is dispersed by a holographic grating with 1800 lines/mm on a Peltier cooled CCD detector (256 × 1024 pixels). The Rayleigh radiation is blocked by notch filters BraggGrate™ (OptiGrate), which allow collecting signals from 10 cm⁻¹ from laser line. The laser power reaching the sample can be limited through the use of neutral density filters. The entrance slit was set at 150 microns. Spectral resolution is ~1.5 cm⁻¹ using the 632.8 nm. Spectra were acquired in the range from 100 to 4000 cm⁻¹ using the line at 473.1 nm with the objective 50x ULWD. Laser power of the order of tens of mW was used, averaging 3-4 analysis with acquisition times of 20–160 seconds each, using the filters D1 and D0.6.

Fourier Transform Infrared spectra (FTIR) were recorded with a Thermo Scientific Nicolet iS10 instrument in the 4000–600 cm⁻¹ range, equipped with an ATR accessory with diamond crystal, with a resolution of 4 cm⁻¹, collecting 32 scans. Previously to each sample a background analysis was recorded, and automatically used to correct the measurement.

In depth morphological and microstructural observations were carried out using a stereomicroscope

TABLE 1. Description of the tested mixtures.

Compositional proportions for every mixtures		
Mixture	Components	Ratio (wt/wt)
A	bassanite + demineralized water	(100:55)
B	bassanite + lime putty + demineralized water	(50:50:30)
C	bassanite + rabbit glue + demineralized water	(100:15,5:37,5)
D	bassanite + MgO + demineralized water	(100:10:55)

Leitz Wild M420 at different magnifications in order to observe the surface morphology in detail and a Scanning electron microscope JEOL 5910 LV, source tungsten filament, coupled with X-ray spectrometer (EDS) in dispersion of IXRF-2000 energy. Analyses were conducted in low vacuum. The compositional nature and distribution of elements on sample was investigated by the EDS spectra and maps from 0 to 20 keV. The measurements were carried out on calibrated images to study the dimensions of gypsum crystals in the samples by image analysis. The software ImageJ was used for this purpose.

A NETZSCH STA 409 PC/PG was used for TG-DSC analysis, with N₂ fluxes of 20 and 40 mL/min respectively with a temperature ratio of 20/10.0(K/min)/900.

The flexural and compressive strength were measured according to European Standard (UNI EN 13279-2 2004) (51). Mercury intrusion porosimetry (MIP) were carried out using a Thermo Scientific PASCAL 140 and PASCAL 240.

For each mixture, the open porosity and the pore size distribution were measured. The pressure applied was between 0.1 and 200 MPa; the resolution (pressure) is: 0.01MPa until 100 Mpa and 0.1Mpa from 100 to 200 MPa; the accuracy is >0.2%; the resolution in volume is 0.1 mm³ and the range of measure (radius) is 7.5 – 3.7 × 10⁻³ μm. The sample dimension was about 0.4×0.4×0.8mm (52). Contact angle measurements were performed with Lorentzen & Wetten Type 4-1 instrument. The measurement were executed according to UNI EN 15802:2010 (53).

3. RESULTS

3.1. Spectroscopic and X-Ray diffraction analysis

The characterization of the raw materials and of the mixtures was carried out combining mineralogical (X ray diffraction) and spectroscopic analyses (Raman Spectroscopy and FTIR). Each analysis was performed on three replicates. The mixtures B, C and

D were analysed after the curing time (1month) too in order to verify the effect of the addition of MgO, rabbit glue and lime putty on hardening: gypsum, anhydrite, and brucite were identified in mixture D, while gypsum, calcite, anhydrite and portlandite were found in the mixture B. The presence of brucite Mg(OH)₂ is due to the hydration of MgO during the preparation of the mixture D. A high content of bassanite was put in evidence, in mixture C, as well as the presence of gypsum and anhydrite. According to Elert et al. (54), the presence of bassanite after hardening is due to the action of animal glue as a barrier that inhibits the formation of gypsum.

The presence of calcite and portlandite in mixture B is linked to the process of lime putty hardening. The determination of brucite (mix D) and portlandite (mix B) suggests the incomplete carbonation of lime putty in the samples. This phenomenon could also be present in building materials, for the very low kinetics of carbonation reaction depending on relative humidity, size and geometry of the artefact. In fact, in the case of bulky architectural elements, it is hard to ensure the effective CO₂ diffusion from the atmosphere (55–58). For these reasons, specimens will be allowed to set completely and the same survey will be the object of a next paper. The specimen B and D have been however studied, considering their interest in building material topic and in view of a comparison with completely carbonated specimens.

3.2. Thermogravimetric analysis and Differential Scanning Calorimetry (TG-DSC)

Thermogravimetry analyses (Table 2) confirmed the above-mentioned results highlighting the presence of brucite in the mixture D. The amount of brucite was lower than expected from the amount of MgO in the mixture; probably some of the unreacted MgO worked as an aggregate. Moreover, a small amount of calcite is present in all specimens, due to impurities in the raw materials used to obtain gypsum. A greater amount of calcite was

TABLE 2. The table shows the weight loss during the heat flow.

Sample	TG-DSC Results				
	Weight loss per temperature range (mg)				
	< 120	120–200	200–400	400–600	> 650
Mixture A	-	9.37 (56.41%)	-	-	1.09 (6.62%)
Mixture B	-	5.94 (40.63%)	-	1.05 (7.16%)	2.31 (15.83%)
Mixture C*	-	6.01 (43.79%)	-	-	1.08 (7.85%)
Mixture D	-	8.02 (50.43%)	0.65 (4.08%)	-	1.09 (6.91%)
Compound identified	-	Gypsum	Brucite	Portlandite	Calcite

* In the mixture C an endothermic peak at 364°C was recorded, probably due to the organic additive

identified in the mixture B, which also contains a certain amount of portlandite due to carbonation not yet complete (59).

3.3. Scanning Electron Microscopy observations (SEM)

SEM observations (Figure 1) show the variability of the morphology and size of gypsum crystals, due to the presence and variety of additives. In Figure 1a (Mixture A) the image of typical acicular gypsum crystals is shown, while in Figure 1b (Mixture B) both acicular and rounded crystals are visible, probably due to the presence of both gypsum and calcite, that were also found by XRD analysis. The acicular gypseous crystals were not detected in mixture C (Figure 1c), and only tabular crystals are observable. Finally, the image of the mixture D (Figure 1d) clearly shows the lowering of the dimension of acicular crystals and the appearance of an amorphous matrix embedding the crystals. The elemental distribution on the samples surface is given in Figures 2–4.

Mixture A was not reported because its composition is obvious. On the contrary, in the rest of the SEM-EDS maps some features are evident and they deserve comments. For instance small lumps were observed, possibly due to the non-uniform blending or to the presence of magnesium impurities, even in the case where magnesia was not intentionally introduced (MixC – Figure 3). In particular, in Figure 2 (mixture B) it is possible to observe an accumulation of calcium in correspondence of the flat surface of the specimen.

Thank to SEM images the crystal size distribution was evaluated. In mixtures A, B and D (Figure 5) crystals length is much than the width (Table 3). On the other hand, mixture C presents a smaller difference between length and width of the crystals.

3.4. Vicat needle

The initial setting time and final setting time were measured by Vicat needle using standard UNI EN 13279-2 (51). As described in Figure 6 and in

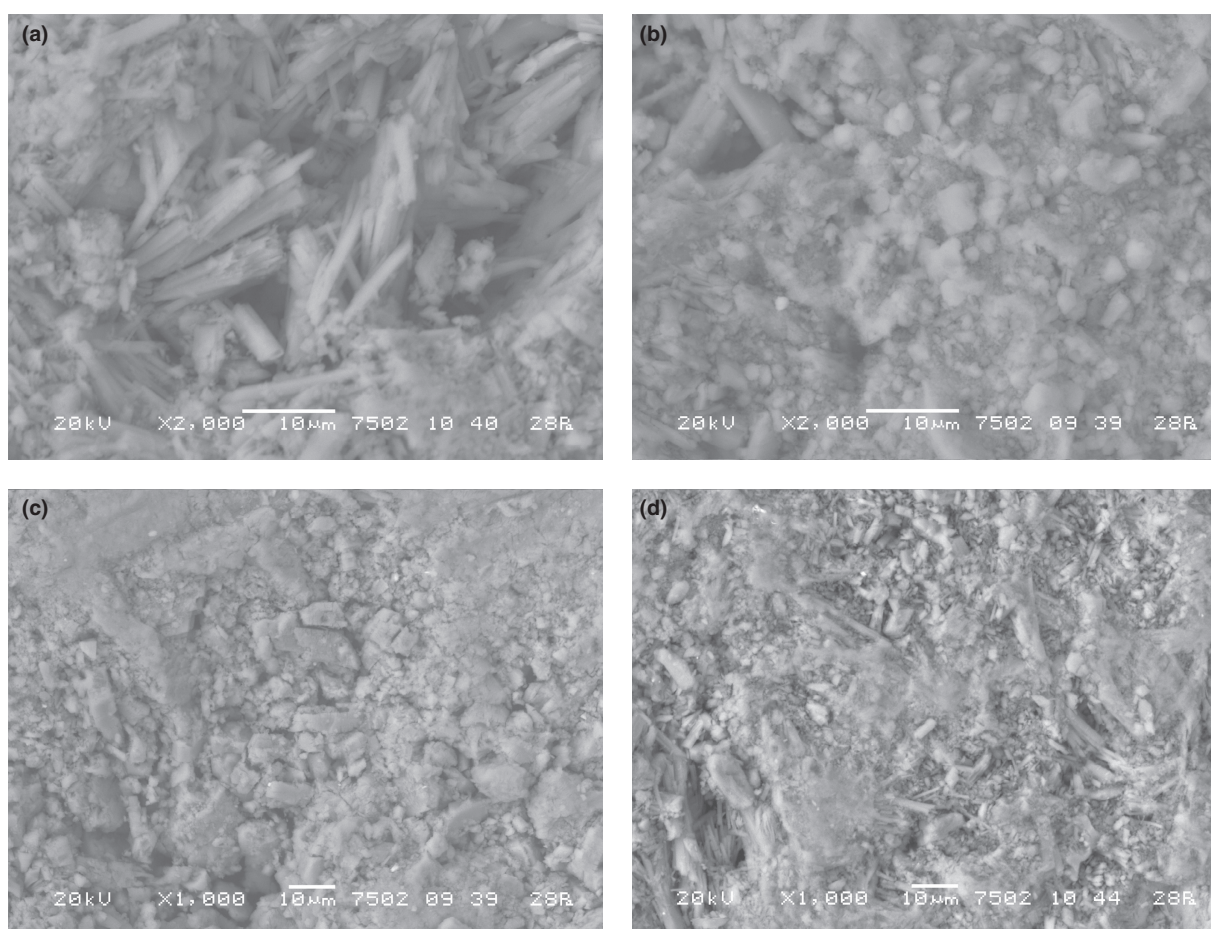


FIGURE 1a, b, c and d. Images of the four gypsum-based mixtures observed by scanning electron microscope (SEM). Bar = 10µm. a) gypsum, b) gypsum and lime putty, c) rabbit glue and d) gypsum and MgO.

Table 4, the comparison between pure gypsum (A) and the mixes B (lime putty) and D (MgO) was interesting. The curves of Figure 6 show the penetration measurements performed by Vicat needle on the mixtures. The time value where the curve starts represents the initial setting time, while the final setting time is reached at the highest value of the curve (PEN. [mm]).

Lime putty and MgO acted as a retardant in gypsum initial setting time. It was also verified that the mixture containing rabbit glue did not provide useful values in Vicat measures because it had not hardened in the measuring range (15h). Anyway, the measure confirmed the role of rabbit glue as strong retardant. This topic will deserve in depth study in the future, with an on purpose procedure overlooking the standard used. It is important to remark that currently no reference values are available for these mixtures, except for pure gypsum used as binder in plastering. In order to comply with the standard EN 13279-1,2, the initial setting time of more than 20 minutes was established (51, 60).

The mixture A showed (Figure 6) the initial setting time at 9.57 min and the final setting time at 14.27 min, corresponding to a penetration value of 37.65 mm. The standard value for the ending point of the final setting time resulted as 40mm, corresponding to the thickness of the sample holder (51). The initial setting times of mixture B (gypsum and lime putty) and mixture D (gypsum and MgO) are around 17.06 minutes and 13 minute, respectively, while the final setting time is around 24 minutes for both of them. The mixture B seems to set quickly, but after the final setting is completed in 10 minutes. This could be considered as a strange performance, surely connected to the presence of lime putty and to its slow hardening due to the carbonation reaction.

3.5. Flow table

The results of workability tests, carried out according to the procedure described in UNI EN 13279-2 2004 (51), showed higher values than those indicated for pure gypsum standards ((165 ± 5) mm) (51).

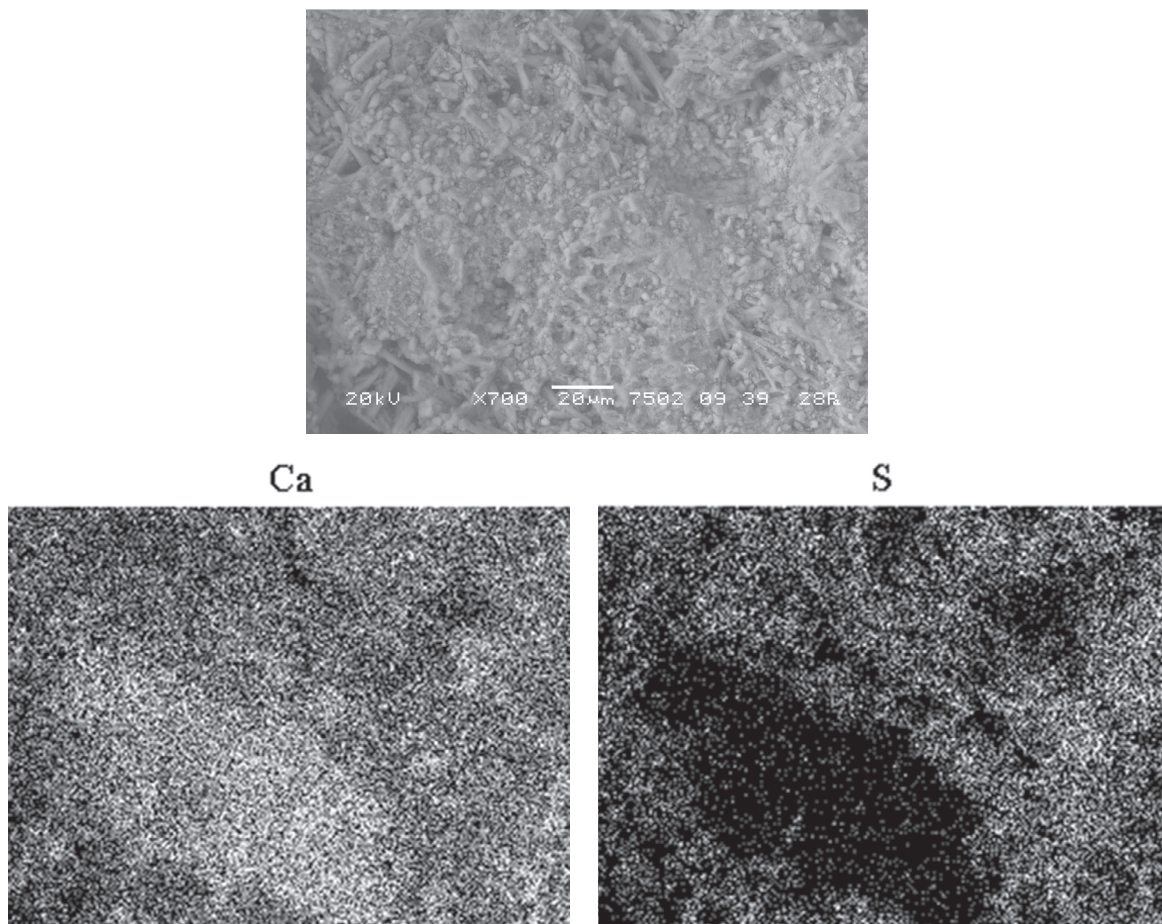


FIGURE 2. EDS maps of the surface of the mixture B: it is possible to observe an area with a greater abundance of calcium and the relative absence of sulphur, suggesting the presence of a lime lump.

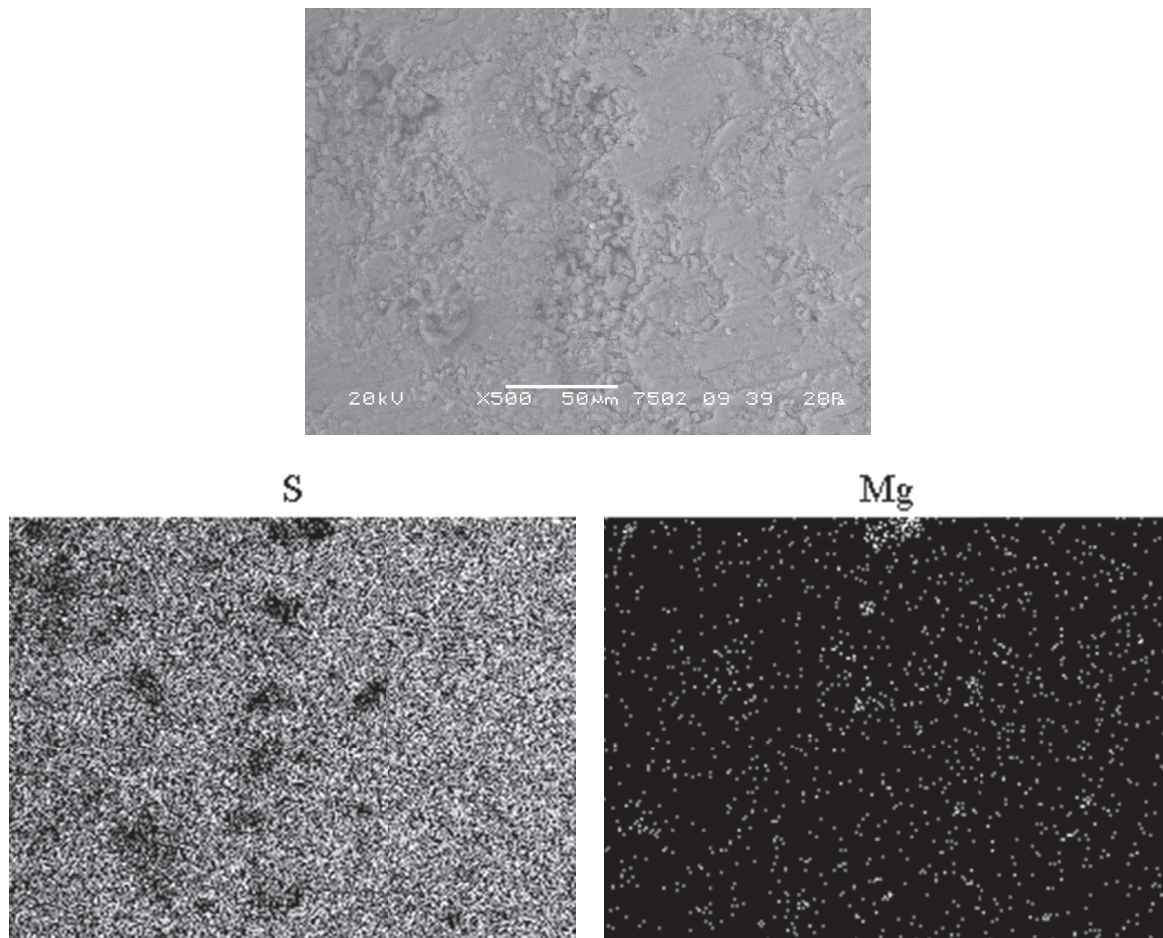


FIGURE 3. EDS maps of the surface of the mixture C, showing the accumulation of Mg in some small areas (max. width of about 50 microns), probably as impurity.

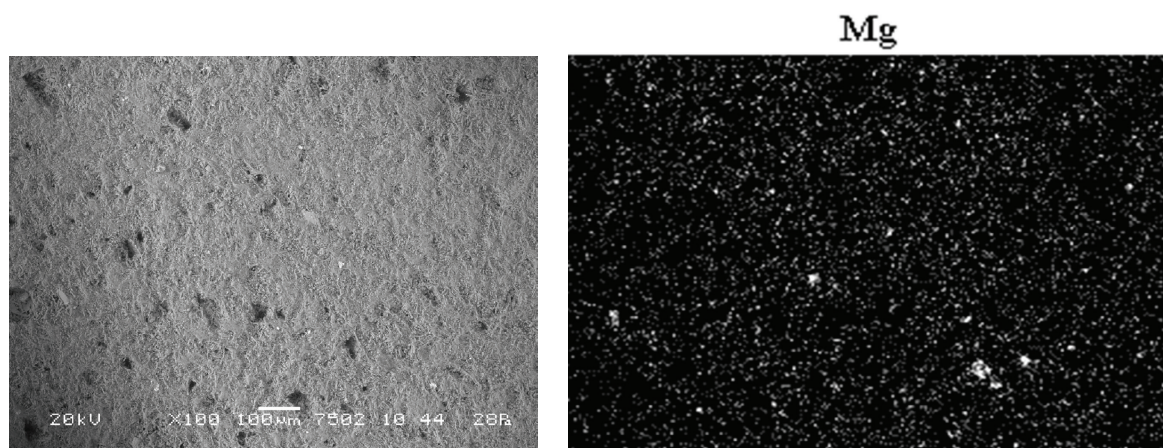


FIGURE 4. EDS maps of the surface of mixture D: some small magnesian lump are evident, probably due a non-uniform mixing.

Moreover, gypsum added with lime putty or rabbit glue seemed to have less workability (Table 5) than gypsum alone [227.5 mm]: 179 mm for mixture B, 170 mm for mixture C and 200 mm for gypsum D.

These mixtures could be used in material integration, re-pointing and other restoration practices. Hence, the workability test proved to provide fruitful results, although they should be

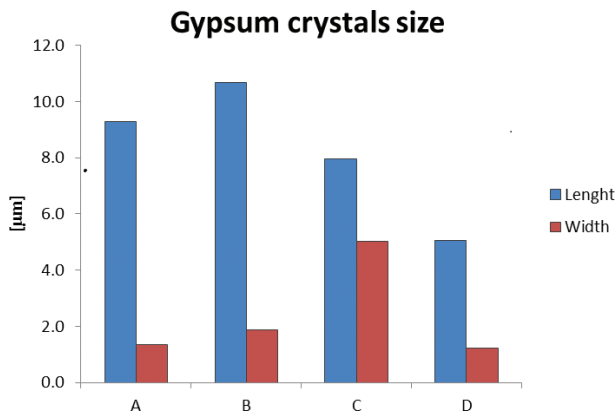


FIGURE 5. Average values of the length and width of gypsum crystals.

TABLE 3. Length/width ratio of gypsum crystals for each mixture type.

	A	B	C	D
Length/Width	6.8	5.7	1.6	4.1

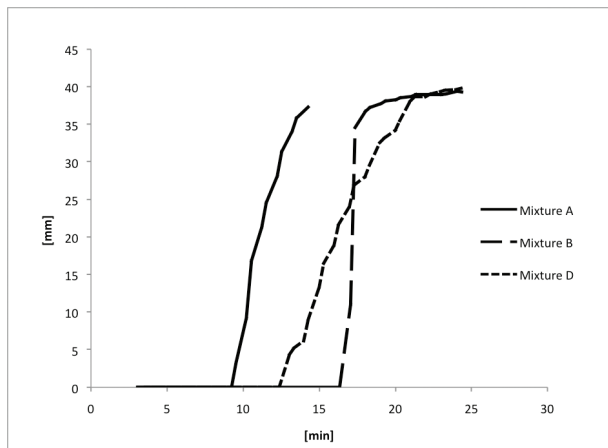


FIGURE 6. Vicat graph shows the initial setting time and the final setting time values for the mixture A, B and D.

TABLE 4. Initial setting time and final setting time of the mixtures A, B and C.

Vicat needle results:		
	Initial setting time	Final setting time
Mixture A	9.57 min	14.27 min
Mixture B	17.06 min	24.06 min
Mixture D	13.09 min	24.32 min

TABLE 5. Flow tables results.

Flow table results		
Flow table	Measured values [mm]	Medium diameter (Ø) [mm]
A Gypsum	230×225	227.5
B Gypsum and lime putty	178×180	179
C Gypsum and rabbit glue	160×180	170
D Gypsum and MgO	200×200	200

performed specifically on a case-by-case basis, in order to better contextualize the needs of each circumstance.

3.6. Mercury Intrusion Porosimetry (MIP)

The porosity values and the pore size distribution are reported in Table 6. The total porosity ranges between 32.7% (mixture C) and 46.9% (mixture B). Mixtures A, C and D show similar values with regard to the average pore radius and in mixture B, the most representative pore class shows a diameter around 1.7 μm. In Figures 7 and 8 the total open porosity and total cumulative volume are plotted versus the pore radius, clearly showing that mixture B has a different microstructure than the other mixes. This behaviour is also shown in Figure 9, where the pore size distribution is plotted versus the relative volume and the pore radius (μm). The results of mixture C are quite interesting, as it appears to be the only one to have a bimodal pore size distribution (Figure 9). As expected, the organic additive filled the inorganic matrix reducing the total open porosity to the lowest value of 32.7%. Moreover, the bulk density resulted to be the highest of the ones measured. The literature corroborates the findings, even if it refers to lime mortars with organic additives (61, 62).

3.7. Flexural and compressive strength

Mechanical tests have been carried out on the hardened mortars after 28 days of curing time, as suggested by standards (51). The measured values are reported in Tables 7 and 8.

The results of flexural strength measurements are presented in Figure 10. The mixture made with gypsum and lime putty (B) presents the lowest value, due to the incomplete carbonation at the time of the measurement. The mixture C displays values slightly lower than mixture A, while the mixture with MgO (D) is characterised by greater variability, with values both higher and lower than the mixture made of pure gypsum. Figure 11 presents the results of compressive strength (mean values of 6 replicates). It is evident that the addition of MgO highly increases the values of compressive strength, whereas mixture

TABLE 6. Average MIP results.

Mercury intrusion porosimetry results					
Mixture	Total cumulative volume (mm ³ /g)	Bulk density (g/cm ³)	Average pore radius (μm)	Total specific surface area (m ² /g)	Total (open) porosity (%)
A.	369.7	1.2	0.8	1.5	43.7
B.	452.6	1.0	1.7	1.8	46.9
C.	245.6	1.3	0.7	1.6	32.7
D.	297.0	1.2	0.8	2.8	36.7

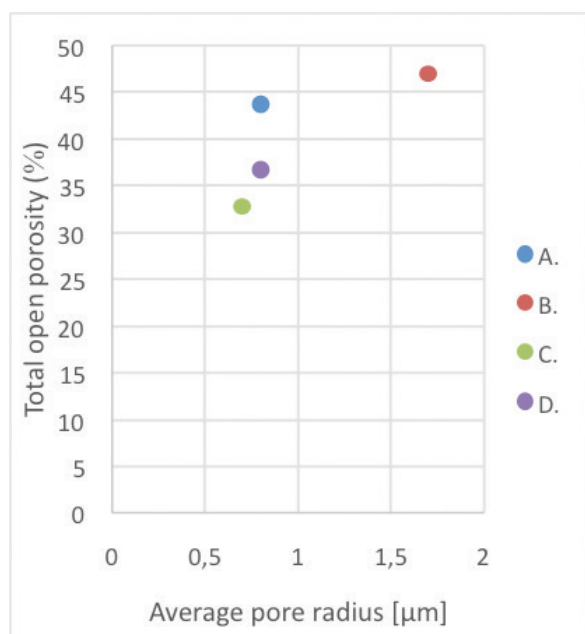


FIGURE 7. The plot shows the average pore radius vs the total open porosity, the plot highlight the differences between mix B and the rest of the mixes.

B shows the lowest result, due to the incomplete carbonation at this stage (63, 64).

3.8. Linear shrinkage

The measures were carried out after 3, 7, 14, 28 days (Table 9). Three specimens for each mixture were analysed as suggested by UNI EN 13454-2 (65). Each mixture expand, generally after an initial shrinking of about 5–10 days, then the dimensions do not vary significantly for the rest of the test. Mixture C shows the maximum difference in size from the starting point to the end of the measurement (-2.41mm). Mixture C is the only one that expands, but remaining below the initial dimensions, with a total effect of shrinkage.

3.9. Contact angle

The contact angle is given by the encounter of the tangent of liquid-vapour interface with a solid liquid interface. By convention, a surface material having a

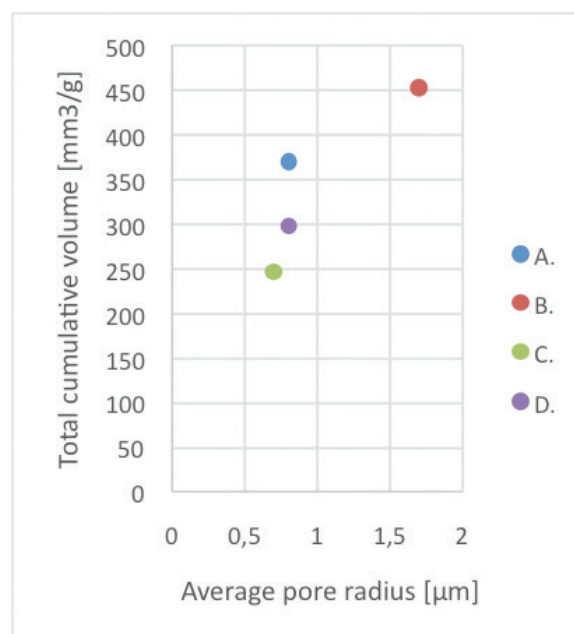


FIGURE 8. The plot shows the average pore radius compared to the total cumulative volume, the plot highlight the differences between mix B and the rest of the mixes.

contact angle with water greater than 90° is defined as hydrophobic, while a surface with angles minor than 90° is hydrophilic. The measurement were performed according to UNI EN 15802:2010 (53). The only mixture on which it was possible to measure the contact angle was mixture C (gypsum and rabbit glue): it resulted as 41° (std. dev. 11). This value does not correspond to a hydrophobic surface, even if it allowed the comparison with absorbing properties of the other mixtures. Mixtures A, B and D in fact did not allow any contact angle measurement, due to the very fast kinetic of water drop absorption. We can conclude that rabbit glue induces the variation of the properties of the surface addressing to lower absorption and lower hydrophilicity.

4. DISCUSSION

The results have clarified the characteristics of the gypsum mixtures prepared in this work. The compositional analyses (after 28 days) allowed identifying the chemical and mineralogical composition

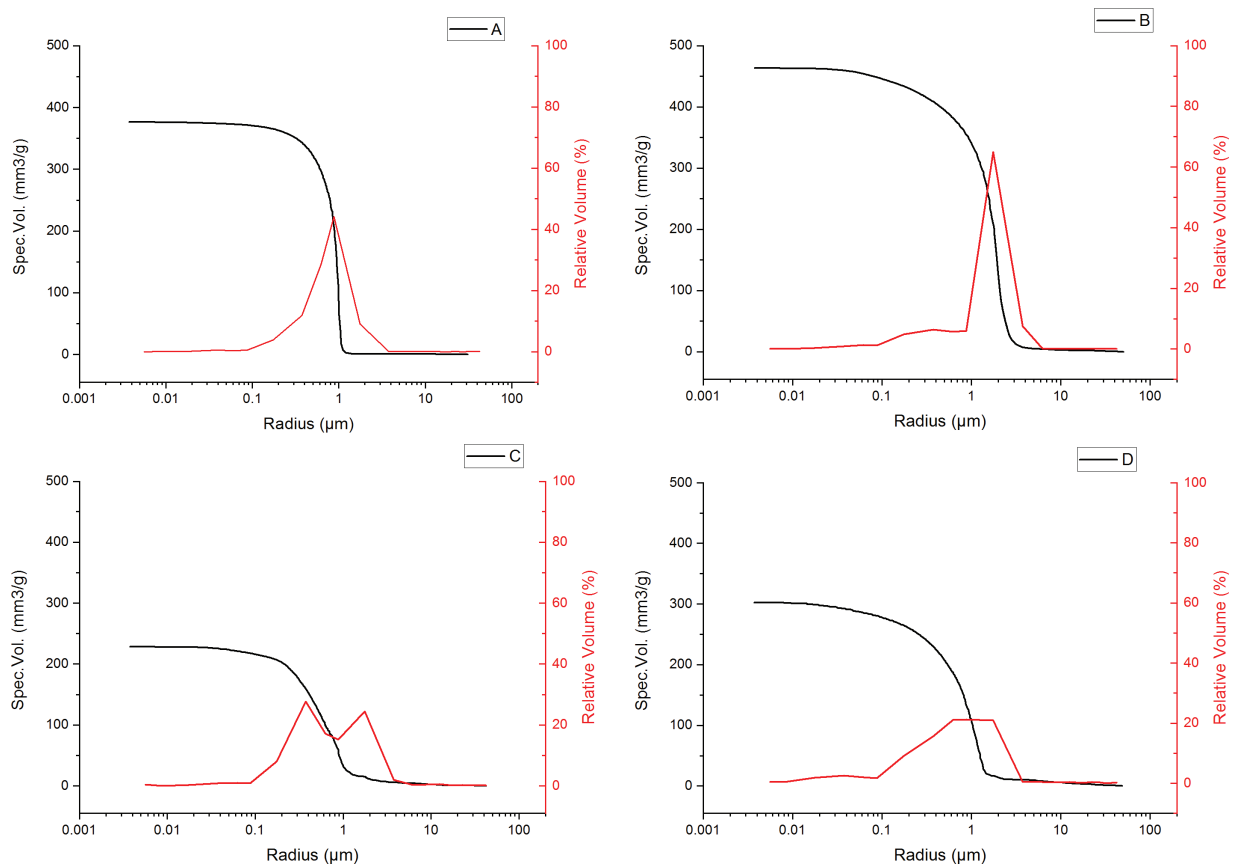


FIGURE 9. Pore size distribution in relation to the cumulative volume and the relative pore volume of the mixture A, B, C and D. Mixes A and B present similar pore size distribution compared to the other mixtures.

TABLE 7. Flexural strength results (MPa).

Specimens	Flexural strength results				Std.dv
	Flexural Strength			Average	
Mixture A	6.62	5.64	6.06	6.11	0.49
Mixture B	2.92	2.84	2.50	2.75	0.22
Mixture C	5.03	5.27	5.10	5.14	0.13
Mixture D	5.19	8.24	3.68	5.70	2.32

of the mixtures. The mixture made of gypsum and MgO showed the presence of brucite, due to hydration of MgO. It is not possible to hypothesize that this contributes to change the final properties of gypsum, as we have deduced from the analysis of this mixture. XRD analysis has been repeated after 12 months, without detecting any significant change, suggesting that the formation of magnesium carbonate or hydromagnesite displays very low kinetics. Atzeni et al. shows that in 18 months aged lime mortars containing magnesium some magnesium hydroxide and other minerals, for example $MgCO_3$, $MgCO_3 \cdot 3H_2O$ and $Mg_4(OH)_2(CO_3)_3H_2O$,

are present. They also underlined that the formation of hydromagnesite is more favoured compared to magnesium carbonate (64). Dheilly et al. studied the hydration process of MgO in different environmental conditions and reported that the formation of magnesium carbonate is not favoured, while the formation of brucite occurs. The minerals that could be detected after the addition of MgO are brucite, nesquehonite, hydromagnesite and giorgisite depending on the environmental conditions (66, 67). Looking at the compositional analysis, the results here reported highlight that only a part of MgO transforms into brucite. Thus, not all MgO behave as a binder and should be considered as part of the aggregate fraction. These results could explain the improvement of the mechanical properties of this mixture, especially with regard to the compressive strength. The presence of magnesium in the binder may also have improved the mechanical properties, as well documented in lime mortars' studies (64, 67).

As for the microstructure, the mixture gypsum/lime putty showed the highest average values of total porosity and of pore radius. These results could be related to the low mechanical properties measured,

TABLE 8. Compressive strength analysis results (MPa).

Compressive strength results								
Specimens	Compression Strength						Average	Std.dev
Mixture A	18.46	17.84	19.56	19.93	19.99	19.62	19.23	0.88
Mixture B	9.50	11.40	9.32	9.87	14.41	11.96	11.08	1.95
Mixture C	16.55	16.55	14.41	16.55	15.88	16.62	16.09	0.87
Mixture D	31.53	30.04	31.58	29.78	28.20	29.74	30.15	1.27

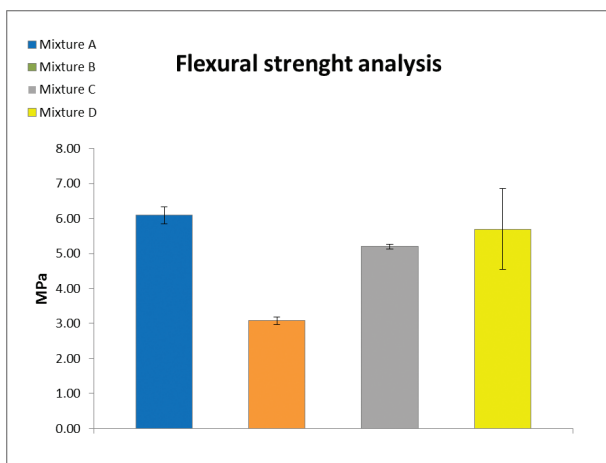


FIGURE 10. Comparison of the flexural strength measurementst after 28 days for mixture A (blue bar), B (orange bar), C (grey bar) and D (yellow bar). The average is calculated on 3 samples.

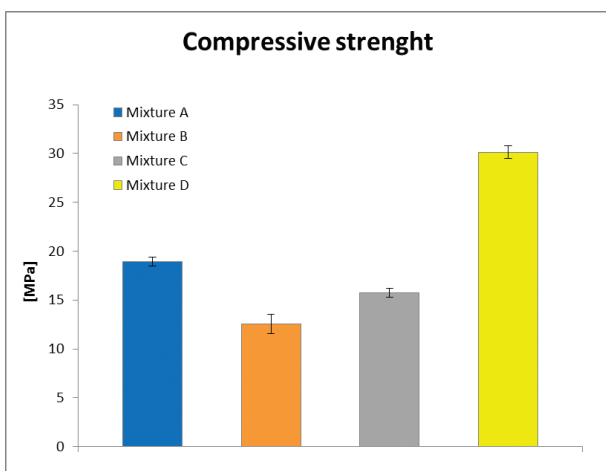


FIGURE 11. Comparison of the compressive strength measurements after 28gg for mixture A, B, C and D; the average is calculated on 6 samples.

even if further analyses are necessary. The presence of portlandite in this mixture is due to the incomplete carbonation of the raw materials, which

TABLE 9. $|\Delta|$ Linear shrinkage [mm] for the four mixtures analysed.

Linear shrinkage [mm]				
Days	Mixture A	Mixture B	Mixture C	Mixture D
3	-0.15	0.12	-3.17	-0.33
7	0.07	0.30	-3.44	0.04
14	0.11	0.46	-2.45	0.23
28	0.18	0.51	-2.41	0.25

probably led to an overall weakness, as resulted from mechanical tests.

Regarding the pore size distribution, mixture B presents pore size distribution % and porosity values similar to mixture A (gypsum), even if the average radius is different. However, the results confirmed the retardant role of lime in setting and hardening mechanisms.

Moreover, the average pore radius in mixtures C and D is closer to the one measured for gypsum in mixture A, although mixture C seems to have a bimodal pore radius distribution (Figure 9). These data should be taken into account when studying the transport phenomena, which are considered crucial when applying fluid products, such as cleaning formulates or consolidants, or in planning filling voids or missing parts with compatible integration materials.

SEM allowed an in depth microstructural survey, which put in evidence the changes induced by the additives, for example those regarding the dimensions and the shape of the gypsum crystals in the mixtures.

The setting and hardening measures clarified that all the additives here considered acted as retardants. An exception to this is the rabbit glue mix, which did not harden at the time of the measurements. Coming to mechanical tests, the mixture including MgO gave an important result: it showed a resistance to flexural strength similar to the gypsum mixture and compression strength higher than each of the other mixtures. As for this mixture, the compressive strength values are higher than the values measured by Sing and Garg in gypsum mortars retardants

increasing it to pH 7 (68). The values here presented are also higher than those measured by Salavessa et al (11), who analysed the mortars after 90 days of curing time, while we measured compressive and flexural strength after 28 days. The comparison with the data reported by Vegas et al (39, 46) shows similar ranking, i.e. the mixture gypsum plus MgO here presented displays higher compressive and flexural strength, with exception of Vegas' sample 10, made with calcium sulphate hemihydrate. Concerning the mechanical analysis of mixture C, we obtained values similar to those of mixture A. Also Elert et al. reported compressive and flexural strength values similar or slightly higher than those measured for mixture made of gypsum and water (54). The mechanical features of mixes containing MgO suggest the use of these materials when a general strengthening is required.

The mixture of MgO and gypsum showed excellent results in the shrinking test too, obtaining a dimensional variation similar to that of pure gypsum. This should be considered a very important result, if we bear in mind the possible application of this material in integration and repointing operations during the restoration practice, because of possible detachment problems. A variation of linear shrinkage slightly greater than that recorded for gypsum was presented by mixture B, while the worst results were obtained in mixture C.

Actually, mixture C is not suitable for injection operations because of its high shrinkage: if used on fragile ancient materials, it could in fact damage or cause cracks in the plaster during the setting and the hardening, especially where the integration is called at filling bulky volumes. Currently it is not possible to compare our results to (42), because no aggregate was added to our mixtures in order to comprehend first of all the features of the binder fraction alone. In any case, we can observe that our results of compressive strength are higher respect to the values reported in (33, 42), even if our samples are more porous. The workability tests provided fruitful results: in fact, as to conservation purposes, the different mixes could be proposed for different final applications and the workability values distributed in a wide range could allow the operator the most suitable choice.

A significant difference in water transport phenomena can be assumed between mixture C and the rest of the inorganic mixes here studied.

5. CONCLUSIONS

When the conservator is using gypsum mixes in integration, embedding or re-plastering operations, very often the ready made products are chosen among those offered by the market. Unfortunately, their composition is not known in most cases. For example, more than one synthetic polymeric

addition could be present. Nevertheless, the habit of preparing on site "on purpose" mixes according to the traditional recipes was lost over the XX century. Hence, empiric knowledge of the properties of these mixes is not very often part of the skills of many conservators. Moreover, even if the general empirical properties are esteemed, normally they have not been measured. In this paper a first approach is attempted and proposed.

This work investigates the effect of three very common additives added in gypsum-based mixtures that acted as retardants. The results obtained from the experimental studies can be summarized as follows:

- The addition of MgO, lime putty and rabbit glue acted as retardant; any of these additives gives time to the conservator of plastering and modelling in relief integration works, proving rabbit glue to be the most retardant compound;
- The mixture made with MgO could provide promising results in restoration practice when a general strengthening is required; anyway, some in-depth studies are needed in order to highlight the possible transformation of Mg compounds in the mix, taking into account that some Mg sulphates may form very dangerous efflorescences.
- The rabbit glue changes the microstructure and the pore network. Most probably, the water transport phenomena could be reduced and a small increase in water repellency could be expected as well, even if some condensation problems on the surface should be considered. In fact, mixture C showed a contact angle of 41° and the material should be considered hydrophilic, but the results interestingly proved the increase of water repellency caused by the addition of rabbit glue. However, more in depth studies are in progress to better understand this aspect.
- A study of the properties of the mixtures after a longer period of curing time could give more information on the characteristic of these materials and their possible applications.

ACKNOWLEDGEMENTS

The authors would like to acknowledge Alessandra Botteon, Mariagiovanna Taccia, Riccardo Negrotti, Cristina Corti and Francisco Jesús Carmona Fernández for their precious contribute in acquiring the data and translation.

Data availability statement

The raw/processed data required to reproduce these findings can be shared on request.

REFERENCES

- Rovero, L.; Tonietti, U.; Fratini, F.; Rescic, S. (2009) The salt architecture in Siwa oasis - Egypt (XII-XX centuries). *Constr. Build. Mater.* 23[7], 2492–2503. <https://doi.org/10.1016/j.conbuildmat.2009.02.003>
- Coppola, M.; Taccia, M.; Tedeschi, C. (2013) Analysis and Conservation of Ancient Egyptian gypsum-based binders and mortars from the temple of Ramesses II in Antinoe. *Built Herit. 2013 Monit. Conserv. Manag.*
- Wilson-Yang, K.M.; Burns, G. (1987) The x-ray photoelectron spectroscopy of ancient murals in the tombs at Beni Hasan, Egypt. *Can. J. Chem. = J. Can. Chim.* 65[5], 1058–1064. <https://doi.org/10.1139/v87-179>
- Ghazi Wakili, K.; Hugi, E. (2009) Four types of gypsum plaster boards and their thermophysical properties under fire condition. *J. Fire Sci.* 27[1], 27–43. <https://doi.org/10.1177/0734904108094514>
- Englert, M.H.; R.B.S.; Sucech, Steven W.; Therese A. Fults; Michael J. Porter; Bruce L. Petersen, R.R.A.D. (2008) United States Patent US 7,364,015 B2. 2.
- Brencis, R.; Skujans, J.; Iljins, U.; Ziemelis, I.; Osits, N. (2011) Research on Foam Gypsum with Hemp Fibrous Reinforcement. *14th Int. Conf. Process Integr. Model. Optim. Energy Sav. Pollut. Reduction, Pts 1 2*, 10.3303/cet1125027. <https://doi.org/10.3303/cet1125027>
- Gaião, C.; De Brito, J.; Silvestre, J.D. (2011) Gypsum plasterboard walls: inspection, pathological characterization and statistical survey using an expert system. *Mater. Construcc.* 62[306], 285–297. <https://doi.org/10.3989/mc.2011.62210>
- Paulo, M. da S.; Veiga, M. do R.; de Brito, J. (2007) Gypsum coatings in ancient buildings. *Constr. Build. Mater.* 21[1], 126–131. <https://doi.org/10.1016/j.conbuildmat.2005.06.035>
- Rampazzi, L.; Rizzo, B.; Colombo, C.; Conti, C.; Realini, M.; Bartolucci, U.; Colombini, M.P.; Spiriti, A.; Facchin, L. (2012) The stucco technique of the magistri comacini: The case study of santa maria dei ghirli in campione d'Italia (Como, Italy). *Archaeometry*, 54[5], 926–939. <https://doi.org/10.1111/j.1475-4754.2011.00651.x>
- Alberti, L.B.; Bartoli, C. (1667) *L'architettura*. Appresso Lorenzo Torrentino, Firenze.
- Salavessa, E.; Jalali, S.; Sousa, L.M.O.; Fernandes, L.; Duarte, A.M. (2013) Historical plasterwork techniques inspire new formulations. *Constr. Build. Mater.* 48, 858–867. <https://doi.org/10.1016/j.conbuildmat.2013.07.064>
- Vitruvius, M.P.; GWILT, J. (1826) *The Architecture of M. Vitruvius Pollio in Ten Books*, Translated from the Latin by J. Gwilt. Priestly and Weale, London.
- Montana, G.; Ronca, F. (2002) The 'recipe' of the stucco sculptures of Giacomo Serpotta. *J. Cult. Herit.* 3[2], 133–144. [https://doi.org/10.1016/S1296-2074\(02\)01169-X](https://doi.org/10.1016/S1296-2074(02)01169-X)
- Igea, J.; Lapuente, P.; Martínez-Ramírez, S.; Blanco-Varela, M.T. (2012) Caracterización de morteros mudéjares de la iglesia de San Gil Abad (Zaragoza, España): Investigación de la tecnología de fabricación de morteros históricos de yeso. *Mater. Construcc.* 62[308], 515–529. <https://doi.org/10.3989/mc.2012.07311>
- Vegas, F.; Mileto, C.; Fratini, F.; Rescic, S. (2010) May a building stand upon gypsum structural wall and pillars?, *8th Int. Mason. Conf. Dresden*.
- Mileto, C.; Vegas, F.; La Spina, V. (2011) Is Gypsum External Rendering Possible? The Use of Gypsum Mortar for Rendering Historic Façades of Valencia's City Centre. *Adv. Mater. Res.* 250–253, 1301–1304. <https://doi.org/10.4028/www.scientific.net/AMR.250-253.1301>
- Pahlavan, P.; Manzi, S.; Sansonetti, A.; Bignozzi, M.C. (2018) Valorization of organic additions in restorative lime mortars: Spent cooking oil and albumen. *Constr. Build. Mater.* 181, 650–658. <https://doi.org/10.1016/j.conbuildmat.2018.06.089>
- Blaeuer, C.; Kueng, A. (2007) Examples of microscopic analysis of historic mortars by means of polarising light microscopy of dispersions and thin sections. *Mater. Charact.* 58[11–12], 1199–1207. <https://doi.org/10.1016/j.matchar.2007.04.023>
- Varas, M.J.; Alvarez de Buergo, M.; Perez-Monserrat, E.; Fort, R. (2008) Decay of the restoration render mortar of the church of San Manuel and San Benito, Madrid, Spain: Results from optical and electron microscopy. *Mater. Charact.* 59[11], 1531–1540. <https://doi.org/10.1016/j.matchar.2007.11.008>
- Gázquez, M.J.; Bolívar, J.P.; Vaca, F.; García-Tenorio, R.; Mena-Nieto, A. (2011) Uso del residuo industrial “yeso rojo” como sustituto del yeso natural para la fabricación de cementos comerciales - Use of the red gypsum industrial waste as substitute of natural gypsum for commercial cements manufacturing. *Mater. Construcc.* 62[306], 183–198. <https://doi.org/10.3989/mc.2011.63910>
- Townsend, J.H.; Doherty, T.; Heydenreich, G.; Ridge, J. (2008) Preparation for Paintings: The Artist's Choice and its Consequences Archetype Books. Archetype Books, London.
- Bustamante, R.; Sánchez de Rojas, M.I. (2007) Study of plaster finishes on San Pedro de los Francos church at Calatayud. *Mater. Construcc.* 57[286], 53–64. <https://doi.org/10.3989/mc.2007.v57.i286.47>
- López-Cruz, O.; García-Bueno, A.; Medina-Flórez, V.J.; Sánchez-Navas, A.; Velilla, N. (2015) Pictorial materials used in the polychrome decorations of the façade of the palace of King Pedro I (The Royal Alcazar of Seville, Spain). *Mater. Construcc.* 65[318], e054. <https://doi.org/10.3989/mc.2015.04314>
- Mayer, R.; Sheehan, S. (1991) *The Artist's Handbook of Materials and Techniques*. Faber & Faber, London.
- Barthe, G.L.; Pinget, A.; Groupe de recherche sur le plâtre (France) (2001) *Le plâtre: l'art et la matière*. Créaphis, Paris.
- Sansonetti, A.; Striova, J.; Biondelli, D.; Castellucci, E.M. (2010) Colored grounds of gill stucco surfaces as analyzed by a combined microscopic, spectroscopic and elemental analytical approach. *Anal. Bioanal. Chem.* 397[7], 2667–2676. <https://doi.org/10.1007/s00216-010-3491-4> <http://www.ncbi.nlm.nih.gov/pubmed/20174784>
- Alessandrini, G.; Bugini, R.; Realini, M.; Sansonetti, A.; Manfredi, G. (2004) A Case Study. The Scala Theatre in Milan: Analysis and Conservation Works on the Facades. In *International Council on Monuments and Sites 10th, International congress on deterioration and conservation of stone*, pp. 785–792.
- La Spina, V.; Mileto, C.; Vegas, F. (2013) The historical renderings of Valencia (Spain): An experimental study. *J. Cult. Herit.* 14[3], S44–S51. <https://doi.org/10.1016/j.culher.2012.11.011>
- Robador, M.D.; Arroyo, F.; Perez-Rodriguez, J.L. (2014) Study and restoration of the Seville City Hall façade. *Constr. Build. Mater.* 53, 370–380. <https://doi.org/10.1016/j.conbuildmat.2013.11.088>
- Paternoster, G.; Rinzivillo, R.; Nunziata, F.; Castellucci, E.M.; Lofrumento, C.; Zoppi, A.; Felici, A.C.; Fronterotta, G.; Nicolais, C.; Piacentini, M.; et al. (2005) Study on the technique of the Roman age mural paintings by micro-XRF with Polycapillary Conic Collimator and micro-Raman analyses. *J. Cult. Herit.* 6[1], 21–28. <https://doi.org/10.1016/j.culher.2004.10.003>
- Rodríguez-Navarro, C. (1988) Binders in historical buildings: Traditional lime in conservation. In *International Seminar on Archaeometry and Cultural Heritage: The Contribution of Mineralogy*. 91–112.
- Charola, A.E.; Pühringer, J.; Steiger, M. (2007) Gypsum: a review of its role in the deterioration of building materials. *Environ. Geol.* 52[2], 207–220. <https://doi.org/10.1007/s00254-006-0566-9>
- Turco, A. (1990) *Il gesso*. Hoepli, Milano.
- Freyer, D.; Voigt, W. (2003) Crystallization and Phase Stability of CaSO₄ and CaSO₄ - Based Salts. *Monatshefte für Chemie / Chem. Mon.* 134[5], 693–719. <https://doi.org/10.1007/s00706-003-0590-3>
- Apostolopoulou, M.; Aggelakopoulou, E.; Bakolas, A.; Moropoulou, A. (2018) Compatible Mortars for the Sustainable Conservation of Stone in Masonries. In *Advanced Materials for the Conservation of Stone*. Springer International Publishing, Cham, pp. 97–123. https://doi.org/10.1007/978-3-319-72260-3_5

36. Pecchioni, E.; Fratini, F.; Cantisani, E. (2008) *Le Malte Antiche e Moderne tra Tradizione ed Innovazione*. Pàtron, Bologna.
37. Cennino Cennini (2009) *Il libro dell'arte*, 5th ed. Neri Pozza, curatore F. Frezzato.
38. Davey, N. (1961) *A History of Building Materials*. Drake Publishers Ltd.
39. La Spina, V.; Fratini, F.; Cantisani, E.; Mileto, C.; López-Manzanares, F.V. (2013) The ancient gypsum mortars of the historical façades in the city center of Valencia (Spain). *Period. di Mineral.* 82[3], 443–457. <https://doi.org/10.2451/2013PM0026>
40. Barthe, G.L.; Pingeot, A.; Groupe de recherche sur le plâtre (France) (2001) *Le plâtre: l'art et la matière*. Créaphis, Paris.
41. Paulo, M. da S.; Veiga, M. do R.; de Brito, J. (2007) Gypsum coatings in ancient buildings. *Constr. Build. Mater.* 21[1], 126–131. <https://doi.org/10.1016/j.conbuildmat.2005.06.035>
42. Igea, J.; Lapuente, P.; Blanco-Varela, M.; Martínez-Ramírez, S. (2013) Design of gypsum-lime based mortars applied on the restoration. In *Science and Technology for the Conservation of Cultural Heritage*, A Balkema Book. Taylor & Francis.
43. Potgieter, J.H.; Potgieter, S.S.; De Waal, D. (2003) An empirical study of factors influencing lime slaking Part II: Lime constituents and water composition. *Water SA.* 29[2], 157–160. <https://doi.org/10.4314/wsa.v29i2.4850>
44. Oates, J.A.H. (2008) *Lime and Limestone: Chemistry and Technology*. Production and Uses Wiley.
45. Rampazzi, L.; Rizzo, B.; Colombo, C.; Conti, C.; Realini, M.; Bartolucci, U.; Colombini, M.P.; Spiriti, A.; Facchin, L. (2008) The stucco decorations from St. Lorenzo in Laino (Como, Italy): The materials and the techniques employed by the 'Magistri Comacini'. *Anal. Chim. Acta.* 630[1], 91–100. <https://doi.org/10.1016/j.aca.2008.09.052> <http://www.ncbi.nlm.nih.gov/pubmed/19068330>
46. Vegas, F. (2013) Parameterisation of Gypsum Mortar for Alternative Structural Consolidation of Traditional Floors. *Adv. Mater.*, 2[4], 48–52. <https://doi.org/10.11648/j.am.20130204.11>
47. Rodríguez, A.; Eremin, K.; Khandekar, N.; Stenger, J.; Newman, R.; Teresa, M. (2010) Characterization of calcium sulfate grounds and fillings of applied tin-relief brocades by Raman spectroscopy, Fourier transform infrared spectroscopy, and scanning electron microscopy. *J. Raman Spectrosc.* 41[11], 1517–1524. <https://doi.org/10.1002/jrs.2824>
48. Ente italiano di normazione (2015) UNI EN 459-1:2015 Building lime - Part 1: Definitions, specifications and conformity criteria.
49. Friess, W.; Lee, G. (1996) Basic thermoanalytical studies of insoluble collagen matrices. *Biomaterials.* 17[23], 2289–2294. [https://doi.org/10.1016/0142-9612\(96\)00047-6](https://doi.org/10.1016/0142-9612(96)00047-6)
50. EN 1015-11: 1999 - Methods of Test for Masonry (1999).
51. Ente italiano di normazione (2014) UNI EN 13279-2:2014 Gypsum binders and gypsum plasters Part 2: Test methods.
52. International Organization for Standardization (2016) ISO 15901-1:2016 Evaluation of pore size distribution and porosity of solid materials by mercury porosimetry and gas adsorption -- Part 1: Mercury porosimetry.
53. Ente italiano di normazione (2010) UNI EN 15802:2010 Conservation of cultural property - Test methods - Determination of static contact angle.
54. Elert, K.; Benavides-Reyes, C.; Cardell, C. (2018) Effect of animal glue on mineralogy, strength and weathering resistance of calcium sulfate-based composite materials. *Cem. Concr. Compos.* 96, 274–283. <https://doi.org/10.1016/j.cemconcomp.2018.12.005>
55. Prasad, P.S.R.; Pradhan, A.; Gowd, T.N. (2001) In situ micro-Raman investigation of dehydration mechanism in natural gypsum. *Curr. Sci.* 80[9], 1203–1207.
56. Liu, Y.; Wang, A.; Freeman, J.J. (2009) Raman, MIR, and NIR spectroscopic study of calcium sulfates: gypsum, bassanite, and anhydrite. In *40th Lunar Planet. Sci. Conf., The Woodlands, Texas*.
57. Sarma, L.P.; Prasad, P.S.R.; Ravikumar, N. (1998) Raman spectroscopic study of phase transitions in natural gypsum. *J. Raman Spectrosc.*, 29[9], 851–856. [https://doi.org/10.1002/\(SICI\)1097-4555\(199809\)29:9<851::AID-JRS313>3.0.CO;2-S](https://doi.org/10.1002/(SICI)1097-4555(199809)29:9<851::AID-JRS313>3.0.CO;2-S)
58. Muyonga, J.H.; Cole, C.G.B.; Duodu, K.G. (2004) Fourier transform infrared (FTIR) spectroscopic study of acid soluble collagen and gelatin from skins and bones of young and adult Nile perch (*Lates niloticus*). *Food Chem.* 86[3], 325–332. <https://doi.org/10.1016/j.foodchem.2003.09.038>
59. Bakolas, A.; Biscontin, G.; Moropoulou, A.; Zendri, E. (1998) Characterization of structural byzantine mortars by thermogravimetric analysis. *Thermochim. Acta.* 321[1–2], 151–160. [https://doi.org/10.1016/S0040-6031\(98\)00454-7](https://doi.org/10.1016/S0040-6031(98)00454-7)
60. Ente italiano di normazione (2008) UNI EN 13279-1:2008 Gypsum binders and gypsum plasters - Part 1: Definitions and requirements.
61. Ventolà, L.; Vendrell, M.; Giraldez, P.; Merino, L. (2011) Traditional organic additives improve lime mortars: New old materials for restoration and building natural stone fabrics. *Constr. Build. Mater.* 25[8], 3313–3318. <https://doi.org/10.1016/j.conbuildmat.2011.03.020>
62. Thirumalini, S.; Ravi, R.; Rajesh, M. (2018) Experimental investigation on physical and mechanical properties of lime mortar: Effect of organic addition. *J. Cult. Herit.* 31, 97–104. <https://doi.org/10.1016/j.culher.2017.10.009>
63. Chever, L.; Pavia, S.; Howard, R. (2010) Physical properties of magnesium lime mortars. *Mater. Struct. Constr.* 43[1–2], 283–296. <https://doi.org/10.1617/s11527-009-9488-9>
64. Atzeni, C.; Massidda, L.; Sanne, U. (1996) Magnesian lime. Experimental contribution to interpreting historical data. *Sci. Technol. Conserv. Cult. Herit.*, 5[2], 29–36.
65. UNI EN 13454-2 Binders, composite binders and factory made mixtures for floor screeds based on calcium sulfate Part 2: Test methods (2007).
66. Dheilly, R.-M.; Sebaibi, Y.; Tudo, J.; Queneudec, M. (1998) Importance de la présence de magnésium dans le stockage de la chaux: carbonatation de l'oxyde et de l'hydroxyde de magnésium. *Can. J. Chem.* 76[8], 1188–1196. <https://doi.org/10.1139/v98-126>
67. Dheilly, R.M.; Bouguerra, A.; Beaudoin, B.; Tudo, J.; Queneudec, M. (1999) Hydromagnesite development in magnesian lime mortars. *Mater. Sci. Eng. A.* 268[1–2], 127–131. [https://doi.org/10.1016/S0921-5093\(99\)00085-4](https://doi.org/10.1016/S0921-5093(99)00085-4)
68. Singh, M.; Garg, M. (1997) Retarding action of various chemicals on setting and hardening characteristics of gypsum plaster at different pH. *Cem. Concr. Res.* 27[6], 947–950. [https://doi.org/10.1016/S0008-8846\(97\)00045-8](https://doi.org/10.1016/S0008-8846(97)00045-8)